

CALCULATING THE LOSS FACTOR OF THE LCLS BEAM LINE ELEMENTS FOR ULTRA SHORT BUNCHES*

A.Novokhatski[#], SLAC National Accelerator Laboratory, Menlo Park, CA 94025, U.S.A.

Abstract

The Linac Coherent Light Source (LCLS) is a SASE 1.5-15 Å x-ray Free-Electron Laser (FEL) facility [1]. Since an ultra-short intense bunch is used in the LCLS operation one might suggest that wake fields, generated in the vacuum chamber, may have an effect on the x-ray production because these fields can change the beam particle energies thereby increasing the energy spread in a bunch. At LCLS a feedback system precisely controls the bunch energy before it enters a beam transport line after the linac. However, in the transport line and later in the undulator section the bunch energy and energy spread are not under feedback control and may change due to wake field radiation, which depends upon the bunch current or on a bunch length. The linear part of the energy spread can be compensated in the upstream linac; the energy loss in the undulator section can be compensated by varying the K-parameter of the undulators, however we need a precise knowledge of the wake fields in this part of the machine. Resistive wake fields are known and well calculated [2]. We discuss an additional part of the wake fields, which comes from the different vacuum elements like bellows, BPMs, transitions, vacuum ports, vacuum valves and others. We use the code “NOVO” together with analytical estimations for the wake potential calculations.

the undulator section (130 m long) the bunch may lose energy due to wake field radiation. Additionally, wake fields may add a significant energy spread to the bunch. If we know this additional energy spread we can compensate linear part of it by changing the phase and the amplitude of an accelerator field in the last linac sections, introducing an opposite energy spread. For better performance the energy loss in the undulator section has to be compensated by varying the K-parameter of the undulators. In LCLS the undulator magnet gap has a small cant angle, which allows remote tuning of K by $\pm 0.6\%$ by small horizontal translations of the undulator magnets [1]. For these reasons we need a precise knowledge of the wake fields in this part of the machine. Additionally we need to know the wake field losses in the 50 m long beam line from the end of the undulator section to the beam dump for a better comparison with the loss factor measurements. These measurements were done using BPMs near the dump.

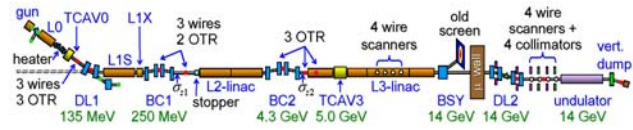


Figure 1: LCLS layout.

INTRODUCTION

An ultra-short bunch is used in the LCLS operation. The bunch is prepared, compressed and accelerated in the main part of the machine, which includes an injector, two bunch compressors and a linac (Fig. 1). Many feedback loops are used in the LCLS operation. The most important loop uses 6 RF phases and amplitudes to control the energy at the four bend systems and the bunch length after each compressor. The bunch length measurement is based on coherent edge radiation from the last dipole of each bunch compressor chicane and each is calibrated in amperes of peak current with the transverse RF cavities. The peak current is stabilized to about 10% rms [1]. The bunch charge is normally held at 0.25 nC and peak bunch current is about 3000 A.

A feedback system precisely controls the final bunch energy (better than 0.04%) up to the region DL2, where the bunch is translated in horizontal direction (Fig.1). DL2 is situated at the beginning of the 300 m long beam transport beam line. This beam line is used to transport the electron beam from the end of the SLAC linac to the FEL undulator (LTU beam line). In this line and later in

BEAM LINE ELEMENTS

The total length of the beam line from the BPM located between the two pairs of magnets in DL2 to the BPMs and YAG screen before the beam dump is approximately 400 m. The LTU beam line is approximately 225 m long and composed of two horizontal dipole magnets (the second pair of magnets of DL2), and a series of quadrupole magnets and correctors. The LTU vacuum chamber contains BPMs, OTRs, and collimators, four types of bellows, vacuum valves, vacuum ports and different kind of transitions. Fig. 2 shows a photograph of a corrector, a bellows and a chamber step. These elements are located after the DL2. Fig. 3 shows photographs of LTU strip-line BPM and a vacuum cross. The main part of the LTU stainless steel vacuum pipe is copper plated. This part is approximately 200 m long. The remaining 25m are a collection of small sections of stainless steel pipe of different cross sections.

The undulator section is 130 m long and contains another type of bellows and BPMs. Fig. 4 shows a photograph of an undulator shielded bellows together with an undulator RF BPM. The vacuum chamber within each undulator segment is highly polished aluminium

*Work supported by Department of Energy contract DE-AC02-76SF00515

[#]nov@slac.stanford.edu

(<0.2- μm surface finish) with a 5-mm height and 11-mm width.

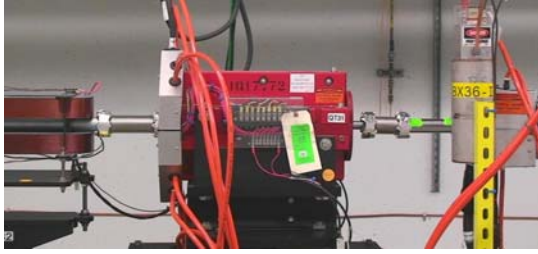


Figure 2: LTU beam line: corrector, bellows, quad, chamber step and bellows.



Figure 3: LTU strip-line BPM. “Lesker” bellows and a vacuum cross.

The dump beam pipe is approximately 50m long and has a stainless steel pipe of larger size.

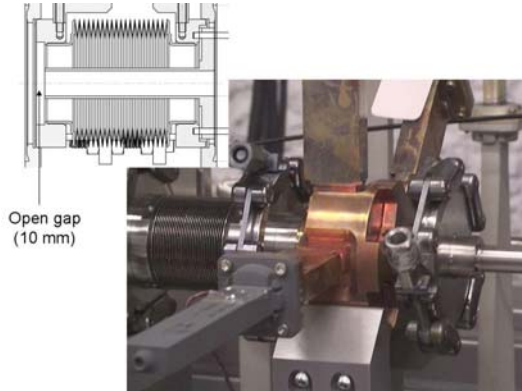


Figure 4: Undulator bellows and RF BPM

Not all vacuum elements produce significant wake fields; however we tried to include each element in our wake field simulation. The beam line elements are specified in Table 1.

WAKE FIELD SIMULATIONS

We use the code “NOVO” [4] for the wake potential calculations. This code can simulate wake fields of very short bunches. We calculate the wake potentials of bellows and BPMs for a bunch length of 2 micron. Using additional analytical estimations [5] we can construct the wake field Green’s function.

Wake fields from the resistive wall pipe with an oxide dielectric layer were calculated using a direct solution of the Maxwell’s equations [6]. Surface roughness wake fields were calculated using synchronous mode model [7].

Table 1: Beam pipe elements from DL2 to dump

Element	Quantity	Description
LTU pumping cross	30	$\phi 34.8$ mm
LTU valves	17	
LTU strip-line BPMs and toroids	27	
LTU collimators	4	
LTU step-out transition	17	$\phi 19.0$ mm
LTU copper pipe		$\phi 34.8$ mm x 190 m
LTU stainless steel pipe		$\phi 19.0$ mm x 30 m
LTU bellows	63	
LTU welded bellows	15	
UND RF BPMs	33	$\phi 10.0$ mm
UND bellows	33	$\phi 10.0$ mm
UND transitions	33	rectangular-to-round
UND transitions	33	round-to-rectangular
UND pumping cross	15	$\phi 10.0$ mm
UND valves	15	
UND aluminium pipe		5 x 11 mm x 120m
DUMP pumping cross	7	
DUMP BPMs	5	
DUMP valves	7	
DUMP stainless steel pipe		$\phi 40.0$ mm x 50 m

To have full comparison with measurements we also include coherent synchrotron radiation (CSR) losses [8] from the two horizontal magnets in DL2 and three vertical bending magnets near the dump.

SIMULATION RESULTS

Four types of bellows are used in the LTU. We simulate wake fields for all of them. Fig. 5 shows the wake field loss factor of the “Lesker” bellows. The photograph of this bellows is shown in Fig. 3. The calculated results show a behaviour of the loss factor with bunch length as a square root function, which agrees very well with an analytical model. An additional bunch energy spread behaves in the same way as the loss factor as a function of bunch length, but with a smaller amplitude (approximately two times).

Wake fields in a shielded undulator bellows are shown in Fig. 6. This kind of bellows has a small gap in the vacuum chamber (Fig. 4) through which the bunch fields penetrate into the bellows convolutions.

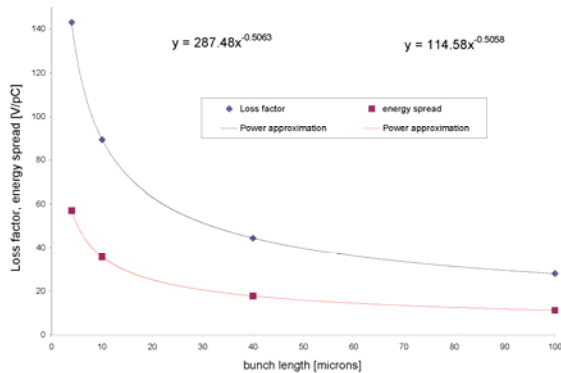


Figure 5: Loss factor of the “Lesker” bellows

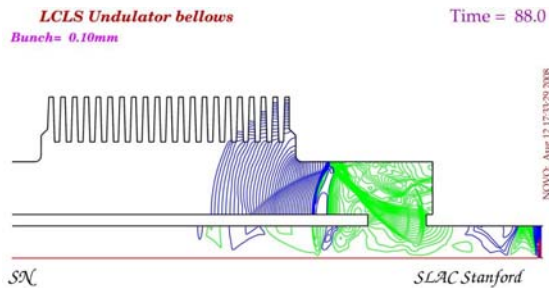


Figure 6: Electric force lines in an undulator bellows

The undulator RF BPM contains two different cavities (Fig. 4), so the loss factor may not be exactly as a square root function of the bunch length.

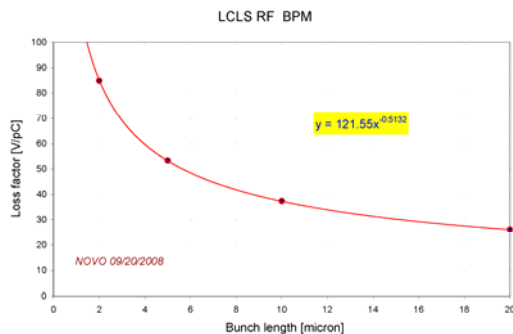


Figure 7: Loss factor of the LCLS RF BPM

But as it can be seen from the calculated BPM loss factor, which is shown in Fig. 7, the difference is not large. We study the effect of the possible oxide layer on the aluminium surface of the undulator beam pipe. Fig. 8 shows the comparison of the wake potentials of a micron bunch in a pure aluminium pipe and a pipe with a 50 nm thick dielectric oxide layer. The amplitudes of the wake

potentials do not differ much for short bunches, but they may strongly differ for longer bunches.

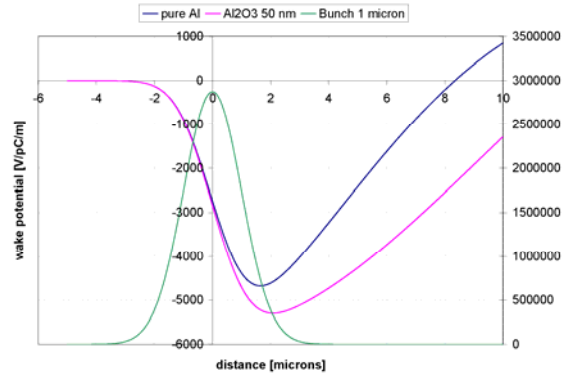


Figure 8: Resistive wall wake field of a micron bunch in a pure aluminium pipe (blue line) and in a pipe with 50 nm oxide layer (pink line).

We note that the transverse wake field has a strong dependence on the thickness of the oxide layer. However the transmission electron microscopy and XPS analysis of a polished aluminium sample of the LCLS undulator chamber showed that the oxide layer is about 4 nm and the surface roughness is of the order of 20 nm [9]. This means that the wake fields due to oxide dielectric layer and surface roughness may be ignored for the LCLS undulator chamber.

The final sum of the loss factor of all beam line elements (specified in Table 1) is shown in Fig. 10 by a yellow line.

WAKE FIELD MEASUREMENTS

In order to measure the wake field loss across the beam line from DL2 to the Dump over the full 400 m distance we use BPMs and the YAG screen at the dump where the vertical dispersion is large. To control the incoming energy jitter we use BPMs, situated in the middle of DL2. We measure the BPM y-position changes in the dump while varying the bunch current keeping constant the bunch charge that is equivalent to varying bunch length. The incoming energy jitter is also subtracted. Detailed information about the measurements is presented in reference [10]. Wake field measurements were done before the undulator magnets were installed. In the presence of undulators we have additionally the spontaneous radiation losses, which can not be avoided. Results of different measurements are shown in Fig. 9. It seems they agree well with a calculated result up to the bunch length of 5 micron. To go to shorter bunches we need to decrease the bunch charge. This may increase the stochastic errors of the BPM readings. CRS effects also will go up with decreasing bunch length, and we don't have good model to simulate this effect right now.

We also tried to make a comparison of the wake field of bunches of different bunch length with the bunch image on the YAG screen near the dump. At least, the wake fields are similar, both increase energy spread with a

smaller bunch length (fig. 10). Bunch charge distributions were calculated by Yuantao Ding [11].

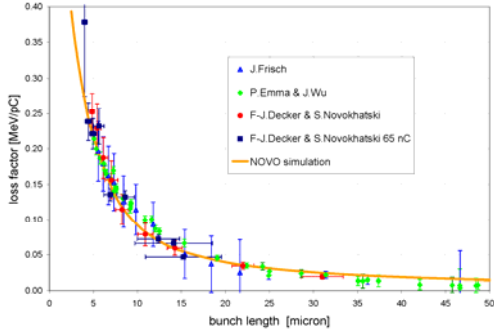


Figure 9: Calculated and measured loss factor.

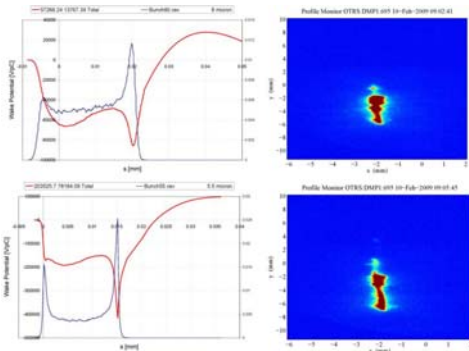


Figure 10: Calculated wake field potentials and real bunch images on a dump YAG screen for the same bunch length.

20 PC BUNCH OPERATION

Successful X-ray generation [12-13] at a very small bunch charge of 20 pC attracted additional attention to the wake fields due to the possibility of measuring the bunch length. Simulation results for the loss factor are shown in Fig. 11. BPM measurements showed that the loss factor from DL2 to the dump may be of the order of 7 MeV, which is smaller than simulated results.

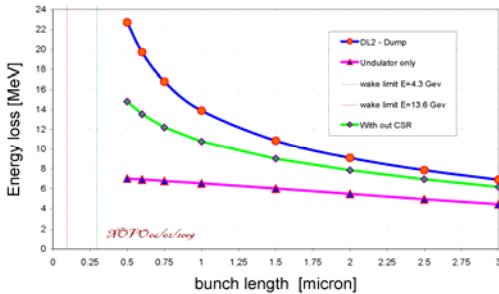


Figure 11: Calculated energy losses or a 20 pC bunch.

However a K-measurement showed a much better agreement with the wake energy losses in the undulator section, about 8 MeV. This number is a little higher than

calculated, but it includes spontaneous radiation as well. Fig. 12 shows the energy loss along the undulator section, calculated from the K-parameters of horizontally translated undulator magnets [14-15]. If we tune the K-parameter by tapering the undulator magnets for the maximum X-ray production, then the wavelength of the undulators must stay constant even as the bunch is losing energy.

In this case we can calculate the energy loss from the K-parameters

$$\lambda(z) = \frac{\lambda_0}{2\gamma^2} \left(1 + \frac{K^2(z)}{2} + \gamma^2 \theta^2 \right) \approx \text{const}$$

$$\frac{\Delta\gamma}{\gamma}(z) = \frac{\Delta K}{K}(z) \times \frac{\frac{K^2}{2}}{1 + \frac{K^2}{2}}$$

The calculated energy loss from this formula is shown in Fig. 12. The linear part of the energy loss must correlate with the wake fields and spontaneous radiation losses. If we subtract the linear part then we will get losses for the X-ray production, which are 7.7 MeV in this case.

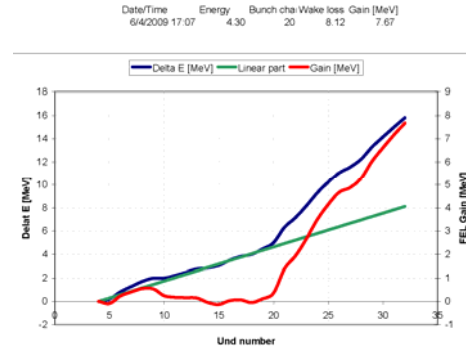


Figure 12: Energy loss along the undulator section.

ACKNOWLEDGMENTS

The author thanks LCLS team for the help of doing this work and measurements of the wake field losses. Special thanks to Mike Sullivan for reading this paper.

REFERENCES

- [1] P.Emma, PAC'09, Vancouver, May 2009,
- [2] K.Bane, G. Stupakov, SLAC-PUB-10707, Sep. 2004.
- [3] P.Emma, Private communication, November 2006.
- [4] A.Novokhatski, SLAC-PUB-11556, Dec 2005.
- [5] A.Novokhatski, Preprint INP 88-39, 1988.
- [6] A.Novokhatski, PAC'09, Vancouver, May 2009.
- [7] A.Novokhatski, A. Mosier, PAC97, Vancouver, 1997.
- [8] J.Murphy et al, Part. Accel. 57, 9 (1997).
- [9] H.-D. Nuhn, Private communication, December 2008
- [10] J.Wu, WEPC24, these proceedings.
- [11] Y.Ding, Private communication, June 2009.
- [12] P.Emma, TUOA01, these proceedings.
- [13] J.Frisch, WEOD01, these proceedings
- [14] H.-D.Nuhn, THOA02, these proceedings.
- [15] J.Welch, THOA05, these proceedings.